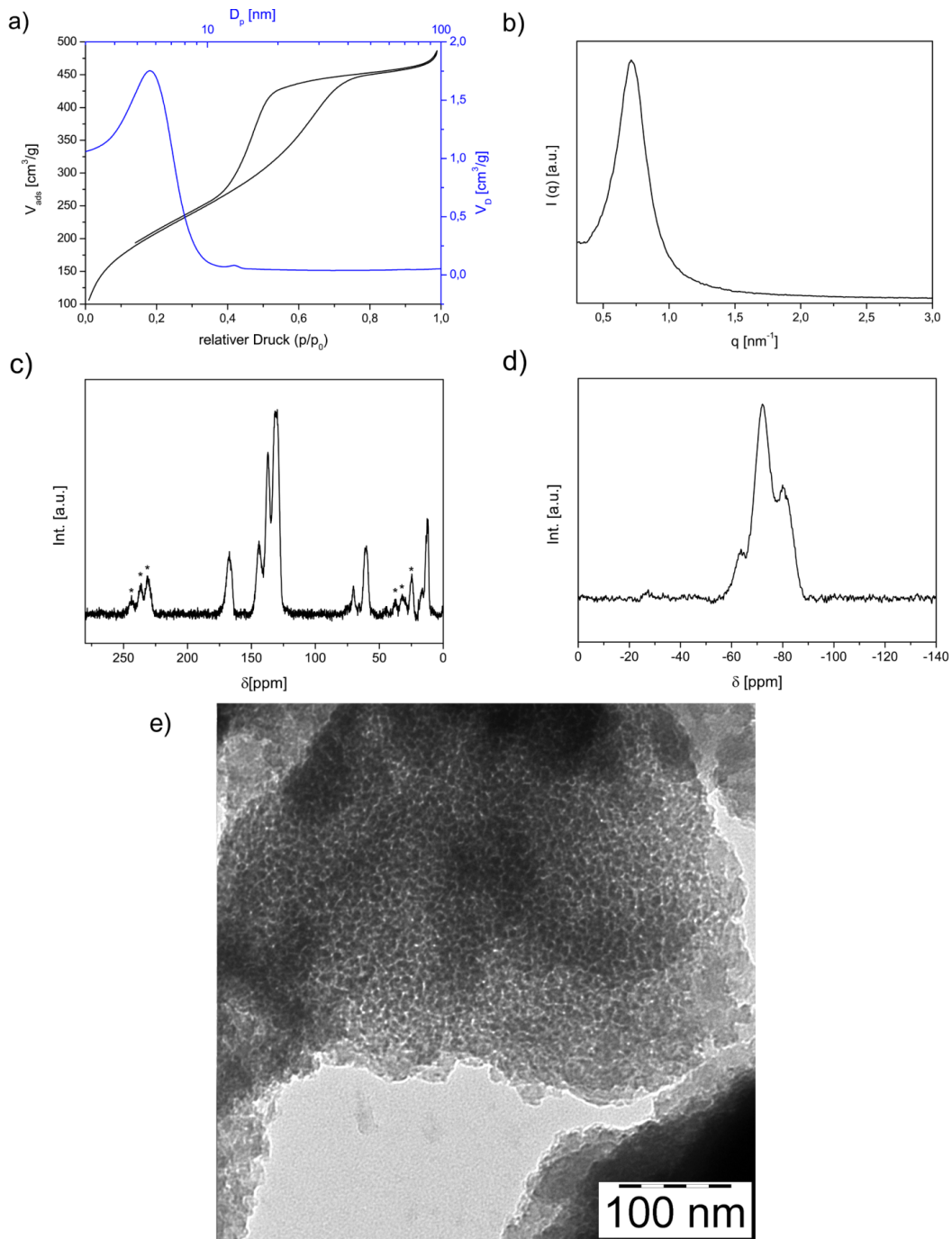


**Multiple Scale Investigation of Molecular  
Diffusion Inside Functionalized Porous Hosts  
Using a Combination of Magnetic Resonance  
Methods**

M. Wessig,<sup>a</sup> Martin Spitzbarth,<sup>a</sup> Malte Drescher,<sup>a</sup> R.  
Winter,<sup>a</sup> S. Polarz<sup>a\*</sup>

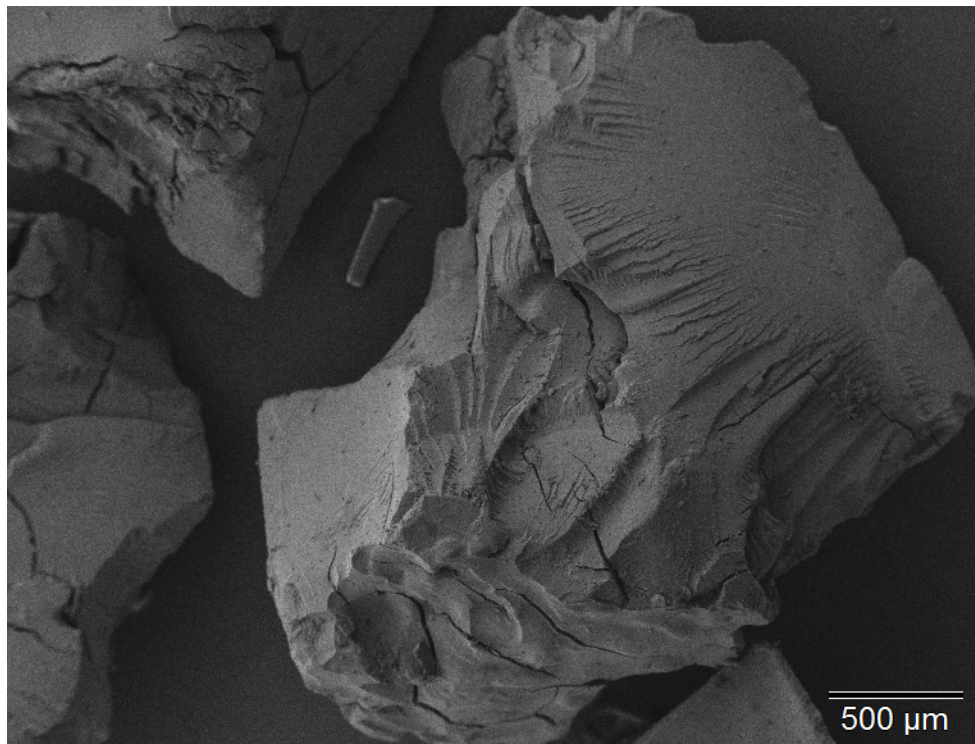
Electronic Supporting Information

## ESI-1. Representative data set for one porous material (UKON2A-56).



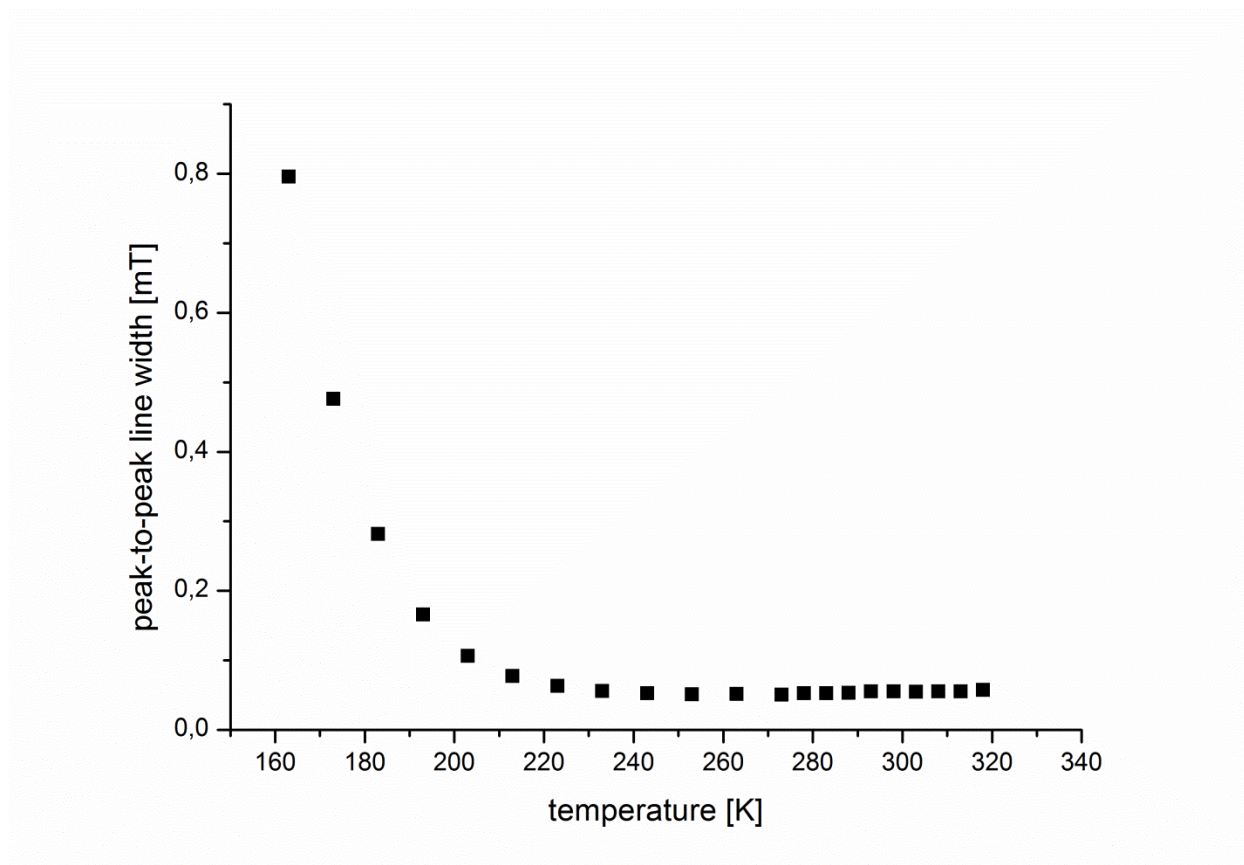
Analytical data of a representative mesoporous material (UKON-2a) containing benzoic acid entities. (a) N<sub>2</sub> physisorption isotherm (black graph) and BJH pore-size distribution function (blue graph), (b) SAXS after extraction, (c) <sup>13</sup>C solid state NMR spectrum with rotating side bands (indicated by \*), (d) <sup>29</sup>Si solid-state NMR spectrum, and (e) TEM.

**ESI-2: SEM micrograph of mesoporous materials with monolithic character.**



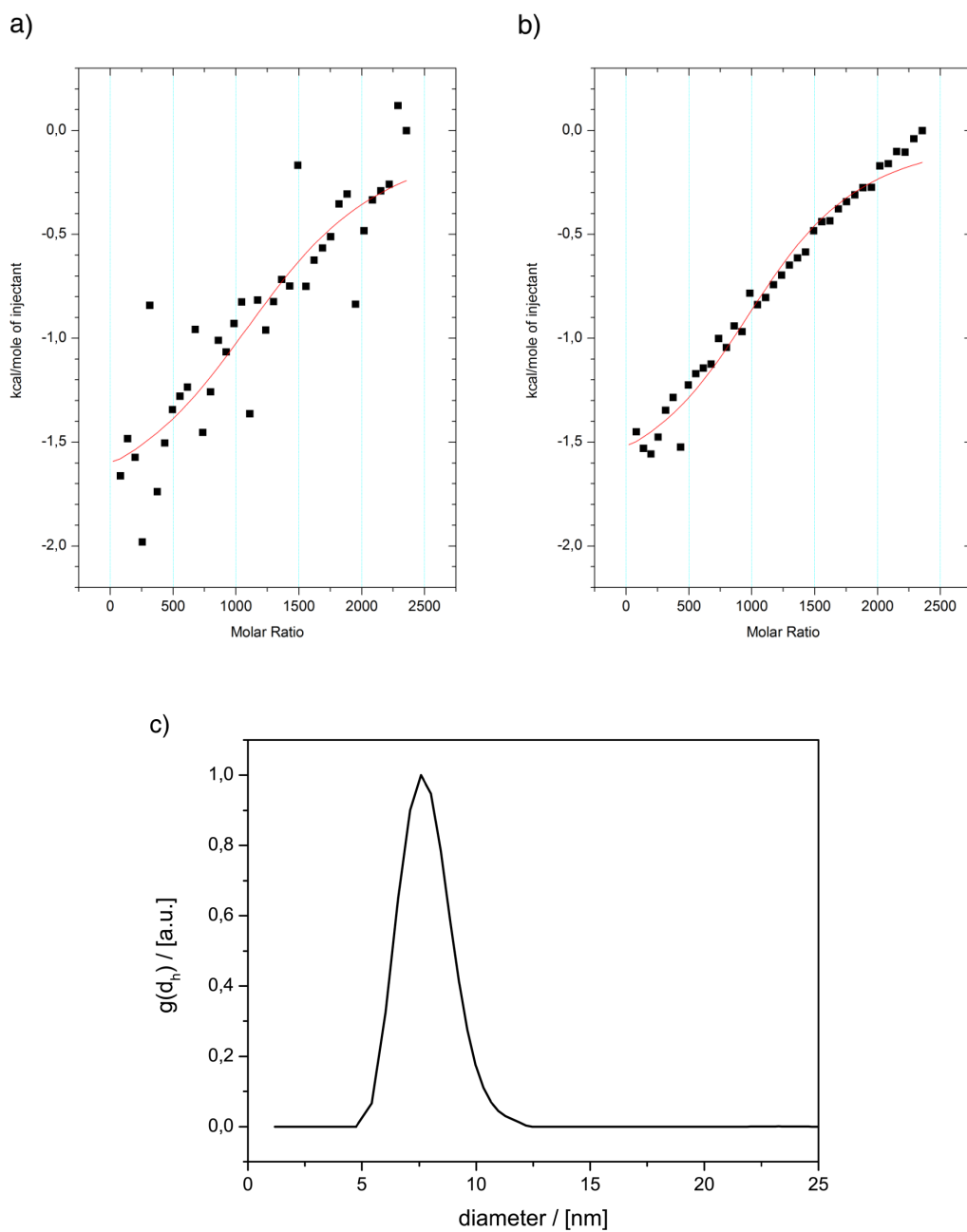
SEM of MPS-54

**ESI-3: Peak-to-peak line width of a 0.5 mM solution of TEMPONE in ethanol.**



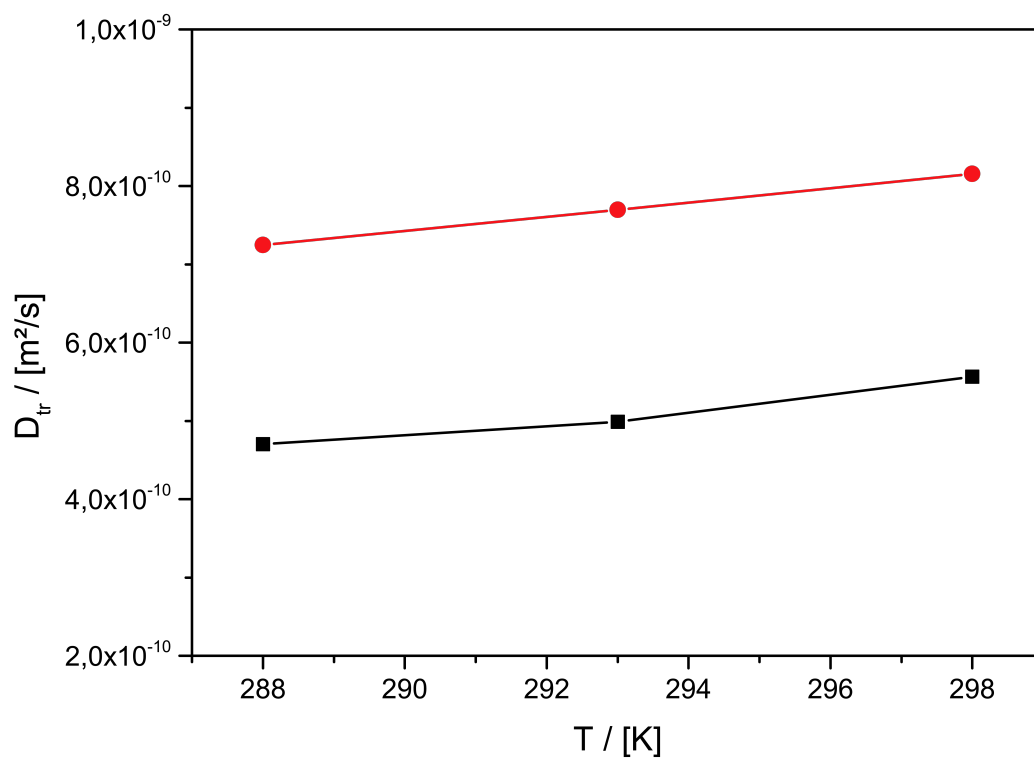
Line width of a 0.5 mM solution of TEMPONE in ethanol at various temperature. For calculating the line width difference  $\Delta\Delta B_c$  only values above 223K have been used since at lower temperature the line width changes drastically due to the higher solvent viscosity.

#### ESI-4: Adsorption studies of TEMPONE and TEMPONE-OH on silica nanoparticles.



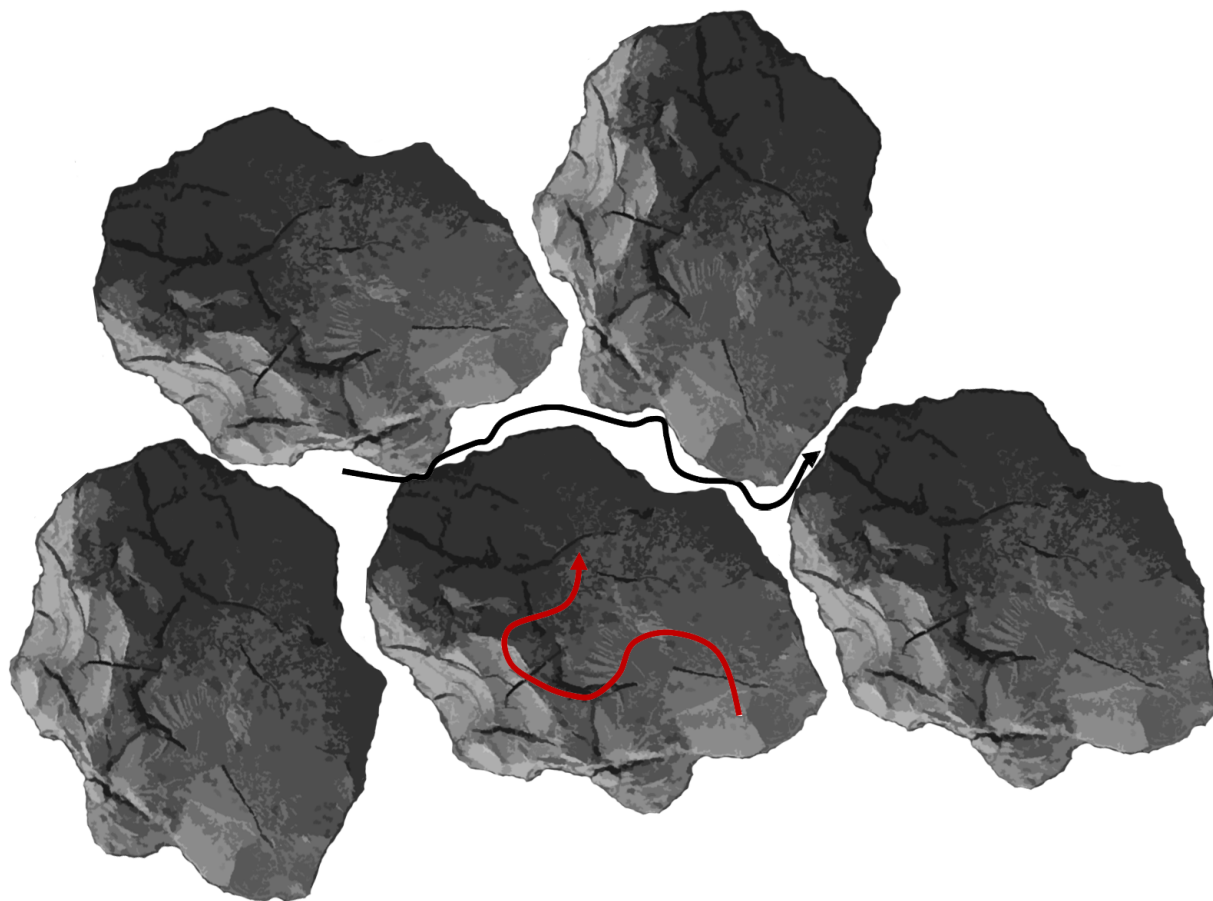
Adsorption enthalpy of a) TEMPONE and b) TEMPONE-OH on silica nanoparticles of 8nm diameter versus the amount of injectant measured by ITC. The molar ratio refers to probe molecules per silica nanoparticle. c) Particle size distribution determined by AUZ of the used silica nanoparticles.

**ESI-5: Temperature dependency of the cw-EPR and MAS PFG NMR experiments.**



**ESI 5.** Diffusion coefficient of TEMPONE (red circles) and TEMPONE-OH (black squares) measured by cw-EPR and PFG MAS NMR respectively.

**ESI-6: Diffusion of molecules between and inside the porous particles.**

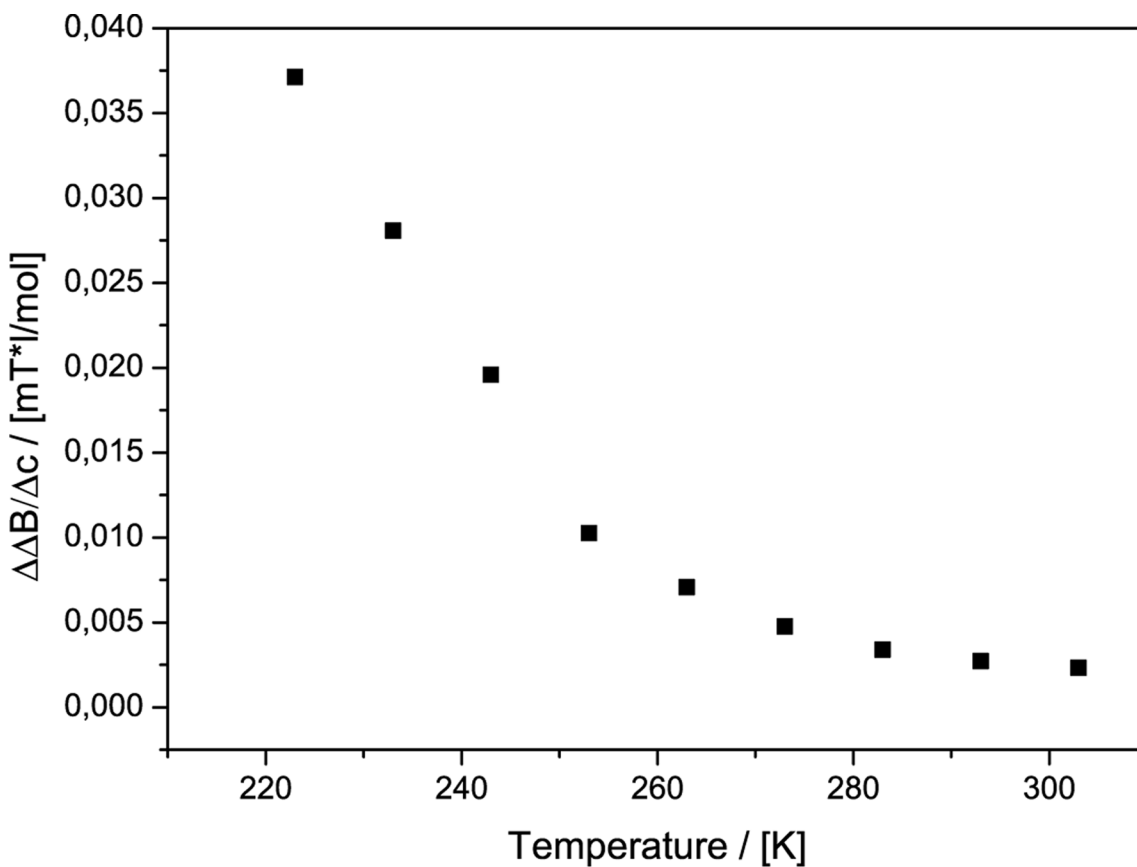


---

**ESI 6.** Assignment of the two component diffusion as seen by MAS PFG NMR. The two components have been assigned to TEMPONE-OH diffusion between (black arrow) and inside (red arrow) the mesoporous particles by its diffusion coefficient.

**ESI-7: Line width difference between a 50mM and 0.5mM TEMPONE solution in MPS-**

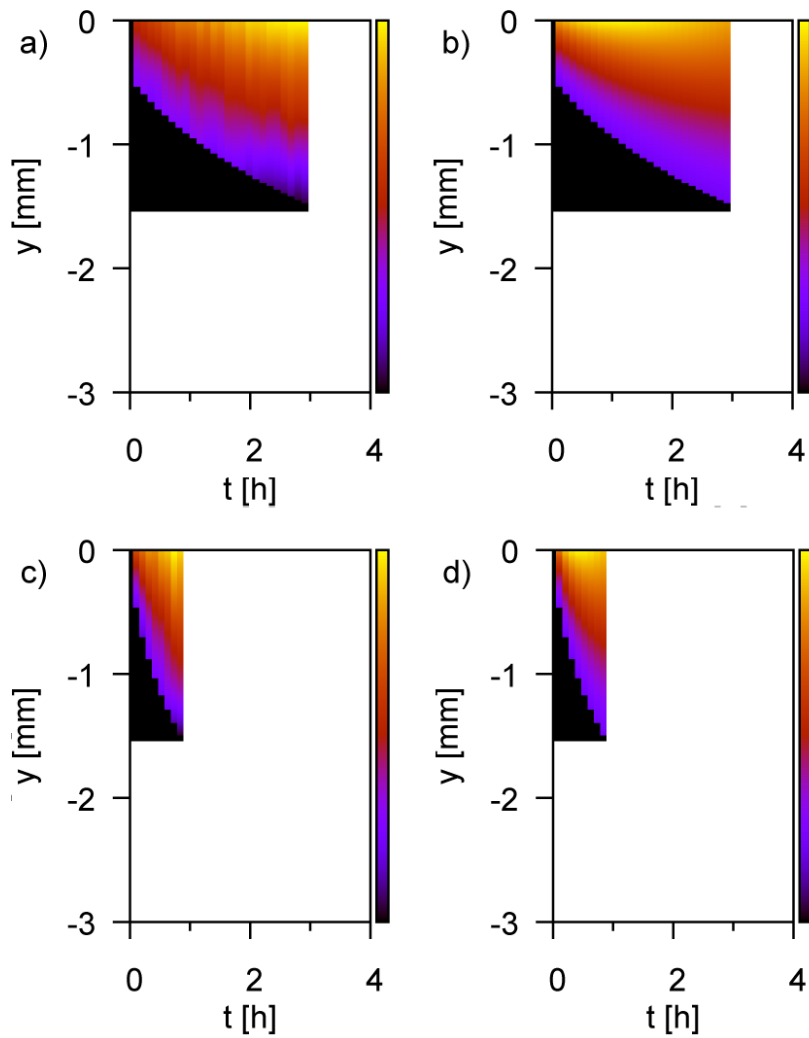
**41M.**



**ESI 7.** Line width difference divided by the concentration difference  $\Delta\Delta B/\Delta c$  of the low field transition at various temperature for MPS-41M. The line width consists mainly of dipole-dipole interaction making it impossible to determine the diffusion coefficient from spin exchange.

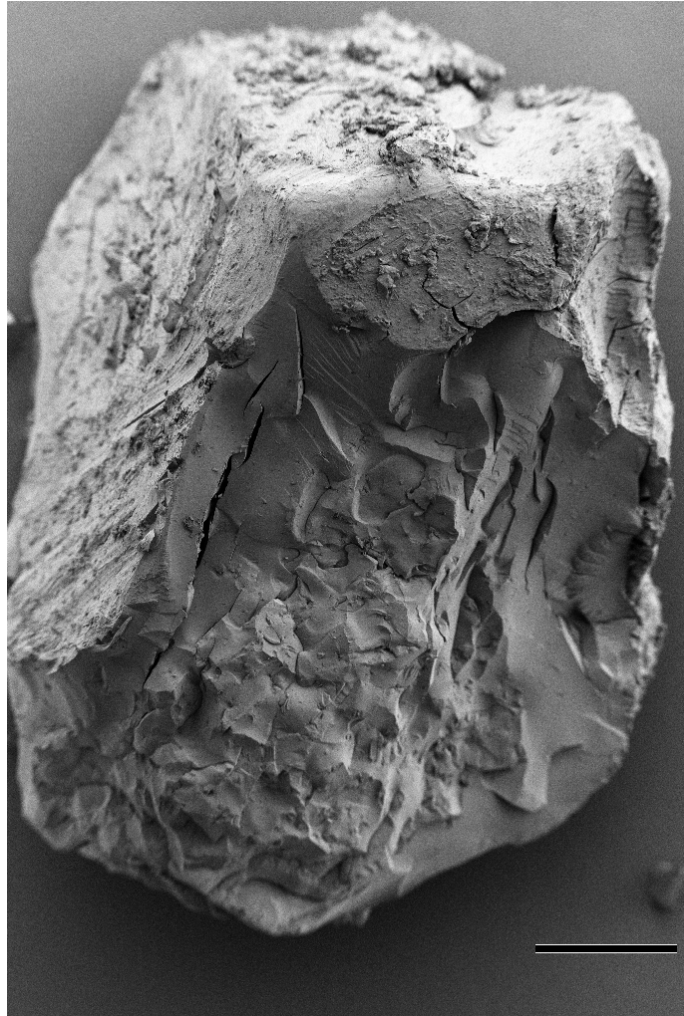


### ESI-8: Diffusion data of MPS-122 and MPOSA-48 from EPR imaging.



Intensity profiles of TEMPONE diffusing from top to down through MPS-54 (a,b), MPS122 (c,d) and MPOSA-48 (e,f) as a function of time. The measured data is always given on the left side (a, c, e), while the simulated intensity profile is given on the right.  $D_{tr, MPS-122} = 2.55(\pm 0.8) \times 10^{-10} \text{ m}^2/\text{s}$   $D_{tr, MPOSA-48} = 1.62(\pm 0.5) \times 10^{-10} \text{ m}^2/\text{s}$  The higher macroscopic diffusion coefficients for MPS-122 and MPOSA-48 compared to their mesoscale diffusion might be attributed to the experimental conditions. We used a shrinking tube to prevent diffusion along the outside of the particles but due to the roughness of the particle surface this might not have been completely suppressed (see ESI-9).

**ESI-9: MPS-122 particle from the EPR imaging experiment after removal of the shrinking tube.**



MPS-122 particle after measuring macroscopic diffusion by EPR imaging and removal of the shrinking tube. The rough surface in the lower part of the particle might have been problematic for contacting with the shrinking tube and therefore excluding diffusion outside the particle.